

Virus replication is not required for oncolytic bovine herpesvirus-1 immunotherapy

Enzo Mongiovi Baracuh,¹ Olga Cormier,^{1,2} Maria Eugenia Davola,^{1,2} Susan Collins,¹ and Karen Mossman¹

¹Center for Discovery in Cancer Research, Department of Medicine, McMaster University, Hamilton, ON, Canada

Oncolytic viruses are a promising approach for cancer treatment where viruses selectively target and kill cancer cells while also stimulating an immune response. Among viruses with this ability, bovine herpesvirus-1 (BoHV-1) has several advantages, including observations suggesting it may not require viral replication for its anti-cancer effects. We previously demonstrated that binding and penetration of enveloped virus particles are sufficient to trigger intrinsic and innate immune signaling in normal cells, while other groups have published the efficacy of non-replicating viruses as viable immunotherapies in different cancer models. In this work, we definitively show that live and UV-inactivated (UV) (non-replicating) BoHV-1-based regimens extend survival of tumor-bearing mice to similar degrees and induce infiltration of similar immune cell populations, with the exception of neutrophils. Transcriptomic analysis of tumors treated with either live or UV BoHV-1-based regimens revealed similar pathway enrichment and a subset of overlapping differentially regulated genes, suggesting live and UV BoHV-1 have similar mechanisms of activity. Last, we present a gene signature across our *in vitro* and *in vivo* models that could potentially be used to validate new BoHV-1 therapeutics. This work contributes to the growing body of literature showing that replication may not be necessary for therapeutic efficacy of viral immunotherapies.

INTRODUCTION

Oncolytic viruses (OVs) are a promising approach for cancer treatment where viruses demonstrate selective cytotoxicity in cancer cells, but not healthy cells, and in many cases induce lasting systemic immunity against the cancer.^{1,2} Although the selective replication of OVs within tumor cells has conventionally been credited for their tumor-killing effects, the induction of host anti-tumor immunity also plays a significant role.^{3,4} We and others have shown that enveloped virus particle binding and entry into normal cells is sufficient to initiate innate immune signaling.^{5–11} Our early studies revealed that non-replicating HSV-1 can induce an antiviral state within cells by inducing the expression of interferon (IFN)-stimulated genes (ISGs).⁹ Further, we showed a diverse collection of enveloped virus particles can induce the expression of ISGs in a mechanism dependent on IFN regulatory factor 3 (IRF3), but not necessarily type I IFN.^{5,7,8,10}

In the broader context of immunotherapy, heat-inactivated (HI) and UV-inactivated (UV) vaccinia virus induce significantly higher

expression of different IFN and cytokines in murine melanoma and dendritic cells, conferring significant survival benefits compared to PBS in mice harboring B16-F10 melanoma tumors.¹² Additional HI vaccinia models induced cytokines, IFN-1, and chemokines in DCs while replicating vaccinia did not, with HI vaccinia being more effective at eradicating tumors than its replicating counterpart.¹³ UV HSV stimulation of human NK cells *in vitro* showed survival benefit in a xenograft mouse model of human acute myeloid leukemia that received administration of these stimulated NK cells,¹⁴ with a follow-up study showing that UV HSV can also stimulate NK cells to lyse prostate cancer cells *in vitro*.¹⁵ Further, the dependency of an OV's efficacy on innate immune signaling is underscored by findings that STING-KO tumors were more resistant to oncolytic HSV-1 than STING-WT tumors.¹⁶ We have previously failed to observe a correlation between the replication of an OV *in vitro* and its efficacy *in vivo*,¹⁷ instead routinely observing an inverse correlation.^{4,17,18}

Bovine herpesvirus-1 (BoHV-1) is an alpha-herpesvirus that can replicate in and kill numerous human immortalized and cancerous cell lines, but not healthy cells.^{19–22} In a study screening the effects of BoHV-1 on the NCI60 panel of established human tumor cell lines, 35% of the panel showed minimal to no BoHV-1 replication, yet still had decreases in cellular viability, which questioned whether replication is required for BoHV-1's anti-tumor efficacy.²⁰ We have shown BoHV-1's efficacy within a therapeutic regimen that induces immunogenic cell death and activates circulating CD8⁺ T cells while reducing infiltration of T regulatory cells.²³ Similar to oncolytic HSV-1, conditions that reduced BoHV-1 replication within tumor cells augmented its therapeutic activity *in vivo*.²³

Taken together, these data suggest that the anti-tumor effects of large DNA enveloped viruses are uncoupled from their ability to replicate. Indeed, it is well appreciated that large DNA viruses encode a plethora of immune evasion genes which may dampen anti-tumor immunity.⁴ To definitively test the hypothesis that oncolytic BoHV-1 replication is not required for its therapeutic efficacy,

Received 27 May 2024; accepted 14 November 2024;
<https://doi.org/10.1016/j.omton.2024.200906>.

²These authors contributed equally

Correspondence: Karen Mossman, Center for Discovery in Cancer Research, Department of Medicine, McMaster University, Hamilton, ON, Canada.

E-mail: mossk@mcmaster.ca



within our therapeutic regimen in a syngeneic melanoma model we tested the single variable of OV replication by comparing live and UV oBoHV-1 particles and observed comparable outcomes in survival. Transcriptome analyses identified overlapping pathways and genes triggered by both treatments. We also present the discovery of a “gene signature” across both *in vitro* and *in vivo* models that may help validate new BoHV-1 vectors and therapy regimens in the future.

RESULTS

Live and UV BoHV-1 induce a small overlapping set of genes in C10 cells *in vitro*

As our previous studies with inactivated virus particles and membrane perturbation were routinely performed in normal (non-transformed) cells,^{5,8–10} we were interested in understanding the gene expression profile of B16-derived melanoma C10 cells infected with either live or UV BoHV-1, using the same number of virus particles. RNA was harvested 6 and 12 h post infection (hpi) and a microarray was used to analyze the transcriptome (Figure 1). The number of differentially expressed (>3-fold) genes increased over time with live BoHV-1, but not UV BoHV-1, consistent with the latter failing to replicate (Figure 1A). The majority of genes expressed by UV BoHV-1 were also expressed by live BoHV-1 (Figure 1A), with this subset of genes remaining consistent over time (Figure 1B), despite differences in relative abundance (Figures 1C and 1D). All but one (Samd9l) of the overlapping genes were ISGs (Figure 1D). UV BoHV-1 only caused the differential expression of 1 unique gene at 6 hpi, cytidine monophosphate kinase 2 (*Cmpk2*; fold change, 3.8), and two unique genes at 12 hpi, guanylate-binding protein 2 (*Gbp2*; fold change, 3.23), and Gm10663 (fold change, –3.26) (Figure 1A).

UV BoHV-1 is as effective as live BoHV-1 at extending survival of tumor-bearing mice

To test the hypothesis that oncolytic BoHV-1 does not require replication for its efficacy, we directly compared live and UV BoHV-1 in a tumor regression study. The schematic for this experiment is outlined in Figure 2A, which is based on our published triple-combination therapeutic regimen that includes low-dose mitomycin C and checkpoint inhibitors programmed cell death ligand 1 (PD-L1) and CTLA-4.^{23–25} Over multiple tumor models, we have validated that mitomycin C at this low dose is immune stimulatory but non-cytotoxic and has no efficacy as a monotherapy or in combination with checkpoint inhibitors.^{23–25} Accordingly, the only variable being tested in this study is the replication capacity of oBoHV-1. C57/Bl6 mice bearing C10 tumors treated with either live or UV BoHV-1-based regimens show no difference in survival. Both groups have significantly longer survival compared with PBS-treated mice ($p < 0.001$; Figure 2B). The average tumor volumes (Figure 2C) and individual tumor growth curves (Figure 2D) of mice treated with either live or UV BoHV-1-based regimens have similar overall growth patterns. Notably, one mouse in the UV group had a complete regression of its tumor, and no tumor developed after a rechallenge of that mouse with C10 cells (data not shown).

Live and UV BoHV-1-treated tumors have similar immune cell infiltration profiles

To evaluate whether UV BoHV-1 within our therapeutic regimen stimulates similar immune cell infiltration as live BoHV-1, mice bearing C10 tumors were treated with either live or UV BoHV-1 following the same therapeutic regimen in Figure 2A. On day 10 after treatment initiation, tumors were harvested and cells were analyzed using flow cytometry (Figures 3 and S1). We noted overall higher immune cell infiltration into tumors treated with the UV BoHV-1 regimen ($p = 0.0014$). Live ($p = 0.0074$) and UV ($p = 0.0159$) BoHV-1 induced significantly more tumor infiltration of CD8⁺ T cells than PBS, while live ($p = 0.034$) and UV ($p = 0.0062$) BoHV-1 induced significantly less tumor infiltration of T regulatory cells compared with PBS. Tumors treated with live ($p = 0.029$) BoHV-1-based regimen induced significantly more infiltration of neutrophils compared with PBS-treated tumors, while tumors treated with the UV BoHV-1-based regimen had similar infiltration of neutrophils compared with PBS. Our UV BoHV-1-based regimen also significantly decreased the infiltration of natural killer cells ($p = 0.0392$). Neither live nor UV BoHV-1 changed the overall infiltration profile of CD4⁺ T cells, macrophages, or natural killer T cells.

Tumors treated with live BoHV-1 + mitomycin C and UV BoHV-1 + mitomycin C have overlapping gene expression and pathway enrichment profiles

To understand at a transcriptional level whether live and UV BoHV-1 + mitomycin C-sensitize tumors to immune checkpoint inhibition in a similar fashion, mice bearing C10 tumors were treated with UV BoHV-1 + mitomycin C and data were compared with previous findings with live BoHV-1 + mitomycin C.²³ Pathway enrichment analysis of the top 10 pathways from each experimental group identified 8 pathways in common between tumors treated with mitomycin C and live or UV BoHV-1, albeit with differences in their ordinal arrangement (Figures 4A and 4B). The pathways associated with chemokine signaling, interleukin-17A signaling, Toll-like receptors, and type II IFN signaling are of particular interest, as these pathways are associated with an immune response. Further, the top 30 differentially expressed genes common between both groups had similar ordinal rankings, indicated in green and red for upregulated and downregulated genes, respectively (Figure 4C).

Identification of a potential gene signature across *in vitro* and *in vivo* models

The failure of *in vitro* oncolytic herpesvirus replication to predict *in vivo* efficacy^{4,17,18,23} currently precludes rapid and effective screening of novel therapy regimens *in vitro*. To see if there is a group of genes that is differentially regulated in C10 cells and tumors treated with mitomycin C and live or UV BoHV-1 across both *in vivo* and *in vitro* contexts, the transcriptome data from all groups were evaluated and compared. Transcriptome analysis of RNA from tumors harvested on day 5 compared with the same *in vitro* treatment groups with RNA harvested at 12 hpi showed 16 genes that were differentially regulated across live BoHV-1 + mitomycin C and UV BoHV-1 + mitomycin C therapeutic treatments, and across *in vivo* vs. *in vitro*

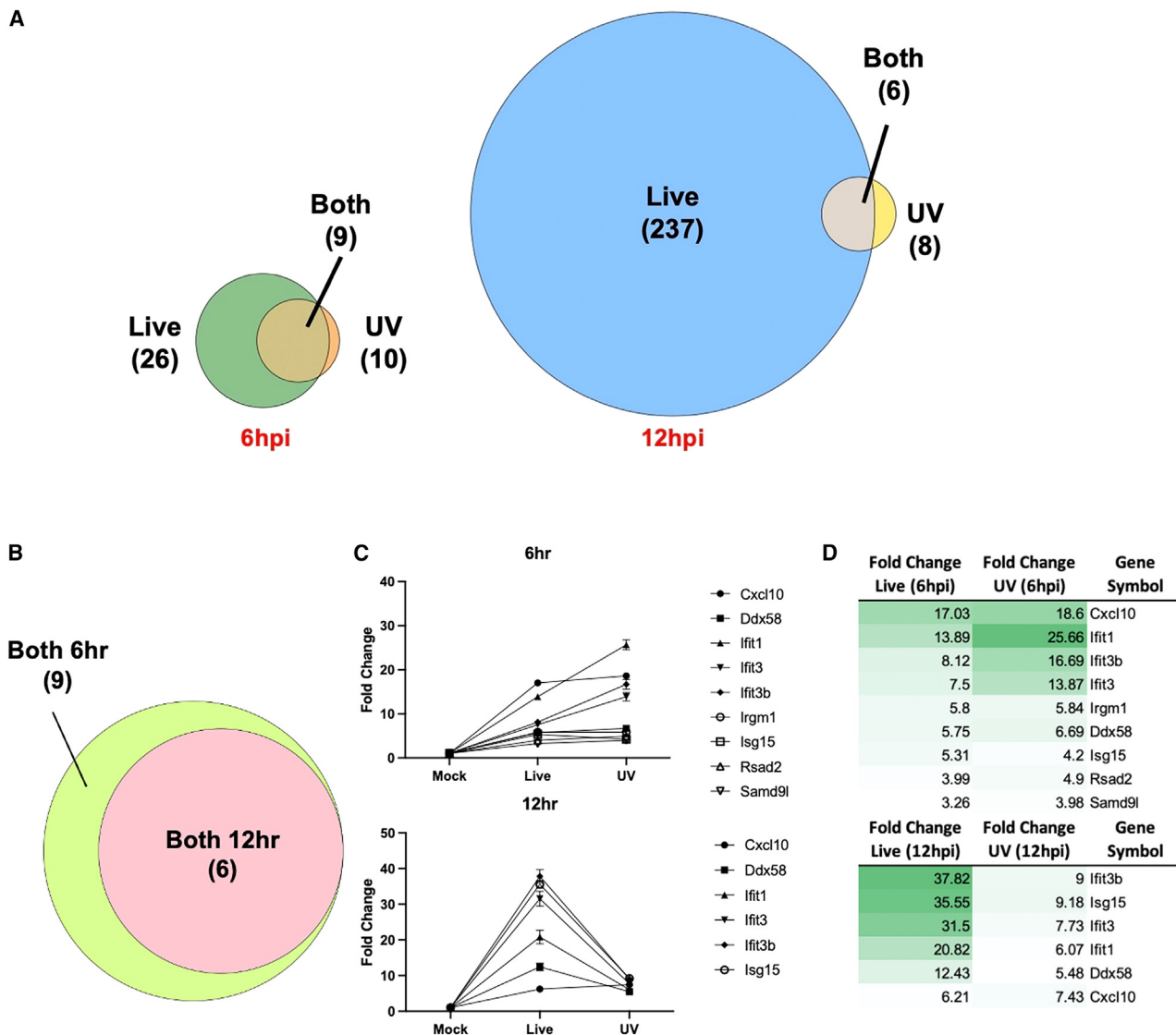


Figure 1. Differential gene expression in C10 cells infected with UV and live BoHV-1

(A) Comparison of genes with differential expression (≥ 3 -fold) induced by live BoHV-1 and UV BoHV-1 at 6 and 12 hpi. (B) Overlap between genes differentially regulated by UV and live BoHV-1 at 6 hpi, with nine shared genes, six of which remain differentially expressed at 12 hpi. (C) Kinetics of relative gene expression between live and UV virus treatments (from (B)), showing similar expression at 6 hpi, but higher expression with live BoHV-1 at 12 hpi. Points on the graphs represent the mean fold change relative to mock and the bars represent the standard deviation. (D) Fold expression values of genes induced by both treatments.

experiments (Figure 5). Ten of these genes are ISGs, many of which are also present in the overlap described in Figure 1, while the remaining 6 genes are related to p53 signaling. Table 1 briefly describes the role of each gene.

DISCUSSION

The overarching dogma that the replication capacity of an OV correlates with its efficacy has been changing with recent preclinical and clinical findings. Here, we directly compared the therapeutic capacity of equal numbers of live and UV BoHV-1 particles within our therapeutic regimen and found no significant differences in tumor control

or survival. The results of the present study align with previous findings showing the efficacy of inactivated viruses for treating cancers in mouse models,^{12,14} and our previous evidence showing a lack of correlation between OV replication and its therapeutic activity.^{17,18} Moreover, a recent report of glioblastoma patients treated with an oncolytic HSV-1 vector showed an inverse correlation between positive patient outcomes and sustained OV antigen expression in tumors.^{44,45} Despite evidence from this and other studies that viral-mediated cell lysis is not necessarily a requirement for anti-tumor efficacy, the field more broadly still refers to these viruses as OVs. However, this term must be used with caution and recognition of

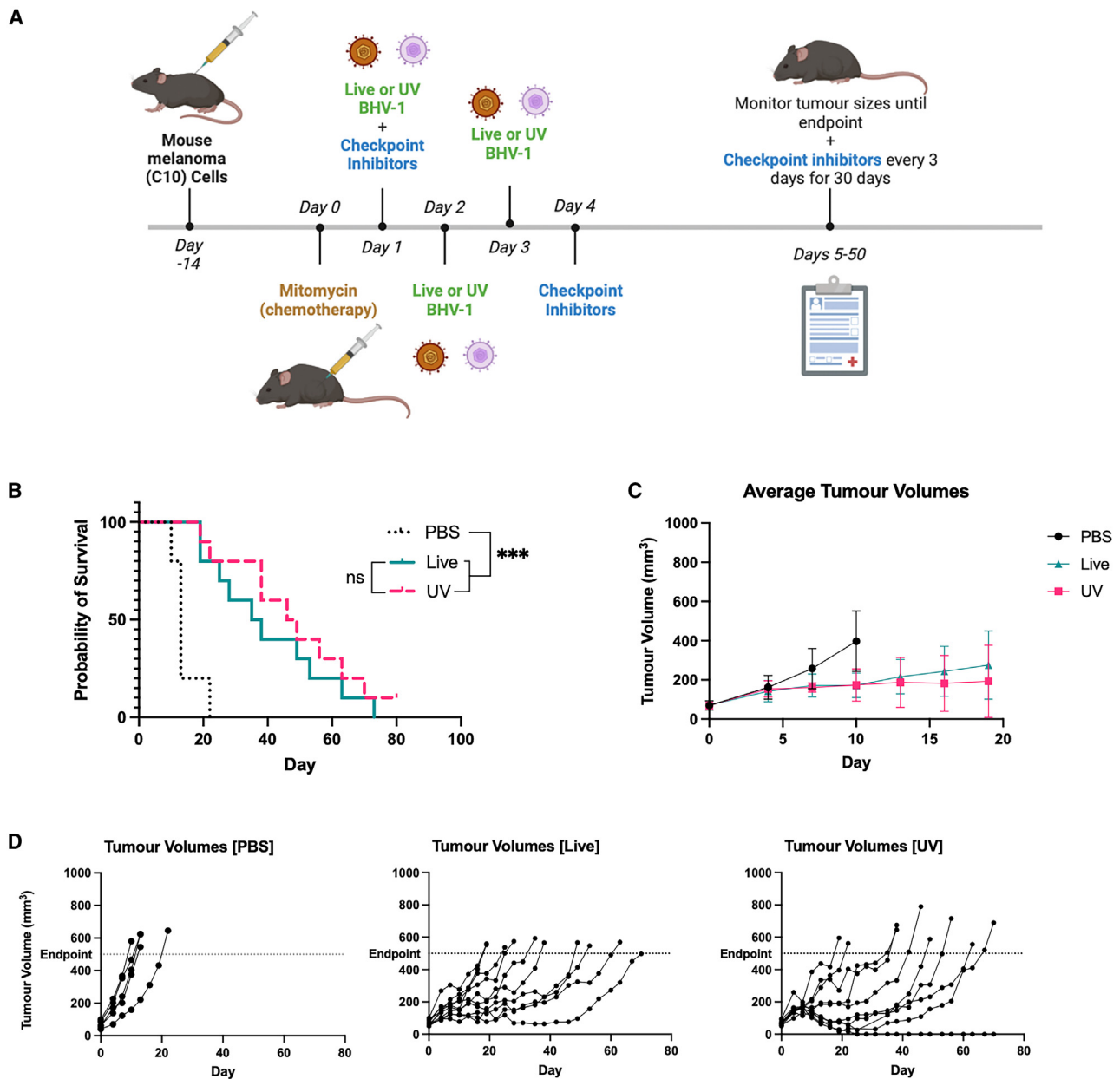


Figure 2. UV-BoHV-1 is as effective as live BoHV-1 at extending the survival of mice bearing C10 melanoma tumors

(A) Experimental schematic outlining the treatment protocol for C57/Bl6 mice with C10 melanoma tumors, treated either with PBS ($n = 5$), live ($n = 10$) or UV BoHV-1 ($n = 10$) as part of a triple-combination therapeutic regimen including mitomycin and checkpoint inhibitors. (B) Survival curve indicating no significant difference in survival between live and UV-BoHV-1-based regimens. (C) Average tumor volumes between groups treated with PBS, live or UV BoHV-1. (D) Individual mice tumor growth curves for PBS, live and UV BoHV-1-treated mice. *** $p < 0.001$.

the caveat that, if there is no “lysis” of cancer cells by the virus, the virus is not truly “onco-lytic.” Thus, it would be more appropriate to refer to these therapeutic viruses that do not cause cell lysis as “viral immunotherapies.” This new terminology is more reflective and inclusive of the biology that involves, and is likely dependent on, stimulation of the host immune system.

Analyses of tumors failed to identify statistically significant changes in tumor infiltration of CD4⁺ T cells, natural killer T cells or macrophages with either live or UV BoHV-1-based treatments compared with treatment, with the simplest interpretation being that these cells are not essential for OV efficacy. In our previous *in vivo* live BoHV-1 regimen study, we observed a trend toward a higher percentage of

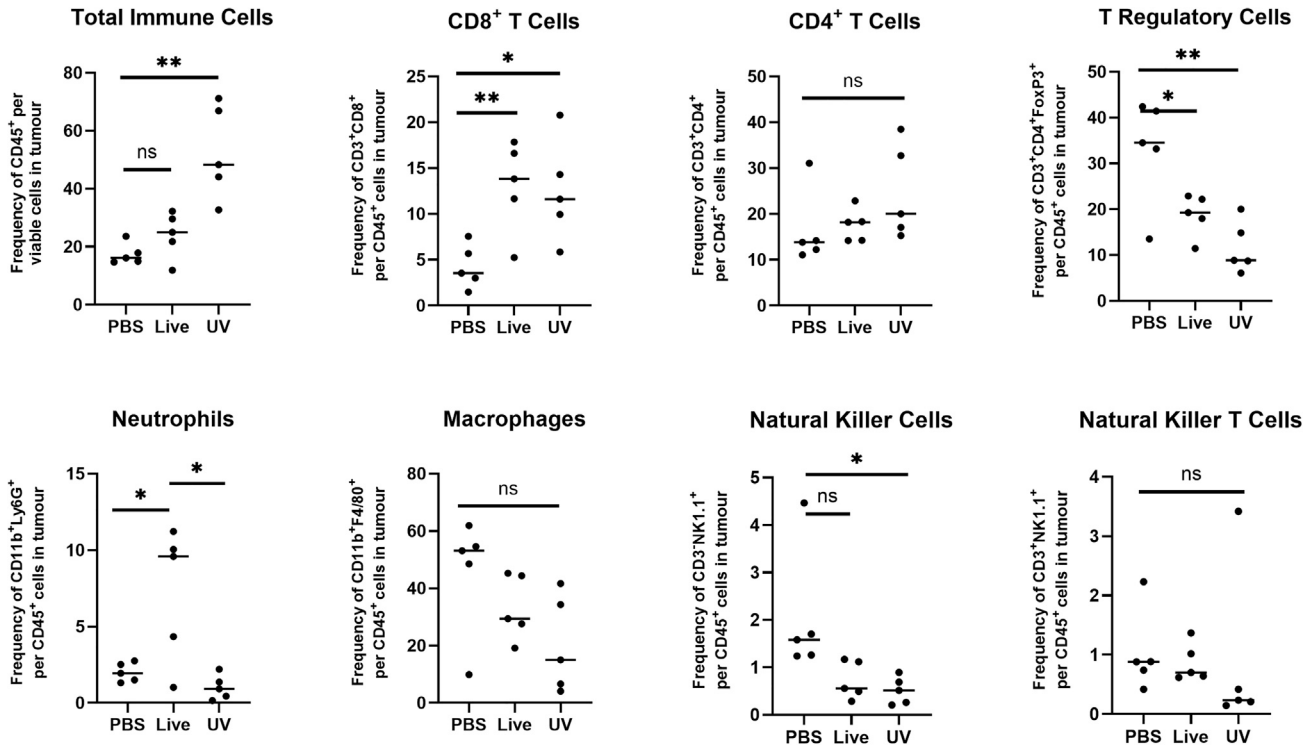


Figure 3. Immune cell infiltration profile of tumors treated with either live or UV BoHV-1-based regimes

Tumors from PBS ($n = 5$), live ($n = 5$), or UV BoHV-1-treated ($n = 5$) regimes were harvested on day 10 (Figure 2A) and analyzed by flow cytometry for the presence of immune cell populations shown as percent (frequency) of immune cell populations per CD45⁺ cells in tumors. Unpaired t test was used for pairwise data comparison. Ns, not significant. * $p < 0.05$, ** $p < 0.01$. Gating strategy is seen in Figure S1.

CD4⁺ T cells relative total tumor cells using quantitative immunohistochemistry of tumor slices,²³ which is a different analysis than performed here. Additional experiments looking at the relative abundance of infiltrating immune cells at different times after treatment along with depletion experiments are needed, as diverse immune cell types have been shown to have anti-tumor effects.^{46–48} The pattern of increased cytotoxic T cell and decreased regulatory T cell infiltration, however, did align with our previous study.²³ These results further support that live BoHV-1 and UV BoHV-1 likely work through similar mechanisms. It is also intriguing that UV BoHV-1-treated tumors show a relative increase in total CD45⁺ immune cells, suggesting that UV virus retains the ability to stimulate immune responses, which may be sustained due to the lack of expression of viral genes with immune-suppressive properties.

Tumor infiltration of neutrophils was notably different between the live and UV BoHV-1 groups. Neutrophil infiltration in tumors treated with live BoHV-1 could be indicative of the host response to replicating virus, as neutrophils have been known to attack virally infected cells.⁴⁹ One study, however, showed that intraperitoneal administration of poly(I:C) in mice increased hepatic neutrophil infiltration as much as replicating virus, which would suggest that viral replication is not necessary for neutrophil infiltration into a tissue.⁵⁰ Thus, it is possible that live BoHV-1 can modulate the immunosup-

pressive tumor microenvironment in a manner that allows for neutrophil infiltration, while UV BoHV-1 cannot. Given that two of five tumors treated with live BoHV-1 had low neutrophil infiltration similar to PBS and UV BoHV-1, it is also possible there is a binary on or off effect of neutrophil infiltration. As there is inherent variability in biological systems, a larger sample size may help to clarify these observations. We and others have shown that neutrophils are a key component of, and sometimes required for, different viral immunotherapies.^{51,52} To our knowledge, however, no other study has yet performed a head-to-head comparison of neutrophil infiltration into tumors treated with a live or non-replicating viral immunotherapy. It is possible that, despite mice being poorly permissive hosts for BoHV-1, virus particles (live or UV) are able to target and modulate immune cells directly, as has been observed in other contexts.⁵³ Additional studies are necessary to further evaluate the significance of immune cell populations in the effectiveness of BoHV-1 immunotherapy.

Pathway enrichment analysis of tumors treated with live vs. UV BoHV-1 suggests that both therapies trigger similar pathways in tumors, despite differences in the total number of differentially expressed genes.^{54–56} Therefore, it is possible that the 63 differentially regulated genes common to tumors treated with live or UV BoHV-1-based regimens represent those responsible for the therapeutic

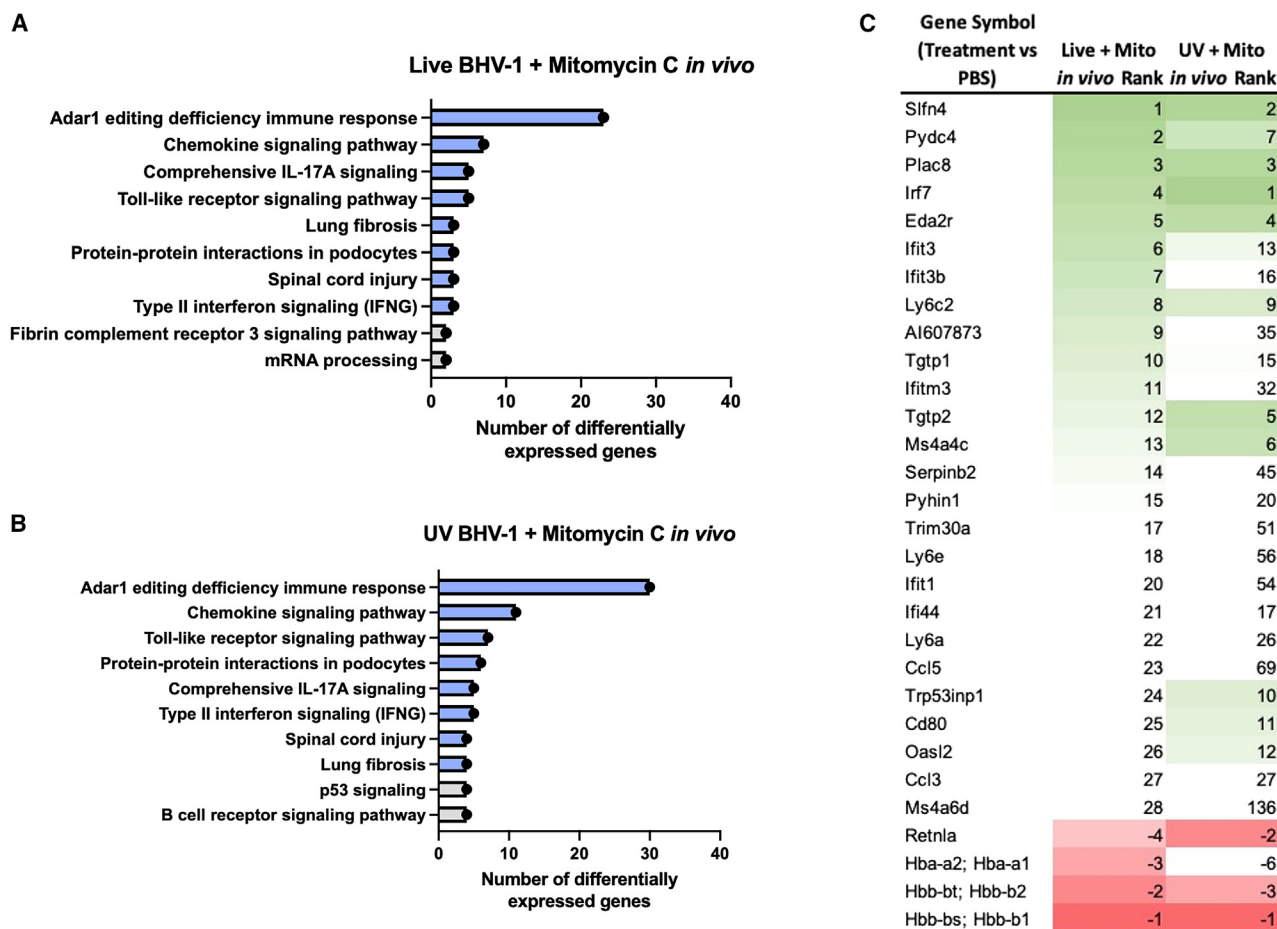


Figure 4. Pathway enrichment profiles and differentially regulated genes of tumors treated with mitomycin C and either live or UV BoHV-1

(A) Histograms of the top 10 pathway enrichment profiles in tumors treated with live BoHV-1 and mitomycin C (Mito) and (B) UV BoHV-1 and Mito. Histograms shaded in blue represent pathways that are in common in both groups. Gray-shaded pathways were identified in both groups, but with ordinal ranks outside the top 10. (C) Ranking of the top 30 differentially regulated genes (>3-fold change) common between tumors treated with Mito and either live or UV BoHV-1. Numbers represent the rank of the relative fold change of each gene. The fold change value for each group is the mean value of five tumors per group ($n = 5$). Green boxes represent upregulation of gene expression and red boxes represent downregulation.

efficacy of BoHV-1. Comparing these enriched pathways and genes in C10 melanoma tumors with those in MC38 (colon cancer) tumors previously treated with an HSV-1 vector with mitomycin C and immune checkpoint inhibitors,²⁴ 6 of the top 10 enriched pathways in that study are among the top 10 in the present study. The notable matching pathways, from most to least enriched, include Adar1 editing deficiency immune response, chemokine signaling pathway, type II IFN response, and Toll-like receptor signaling pathways, which are consistent with viral infections. The Adar1 editing deficiency immune response was the top enriched pathway in all three cases: live BoHV-1, UV BoHV-1, and live HSV-1,²⁴ all with mitomycin C. In a typical non-virally infected cell, the adenosine deaminase acting on RNA (ADAR) enzyme catalyzes the conversion of adenosine to inosine on double-stranded RNAs, which helps cells to reduce the overactivation of dsRNA pathways to avoid autoimmunity.⁵⁶ ADAR1 is IFN inducible and upregulated by many viruses,⁵⁷ while its deficiency is

associated with autoimmune disorders.⁵⁶ In the context of our viral immunotherapy regimens, ADAR1 editing deficiency could be one of the strongest overarching driving factors of tumor killing, allowing for strong expression of ISGs. It is well understood that mitomycin C results in DNA damage, contributes to ADAR signaling, and may trigger both p53- and p21-dependent pathways based on the cell context, so it is unsurprising that we observe transcriptional changes in those pathways in our analyses.^{54,55,58} Overall, these results also illustrate the similarities in the anti-tumor mechanisms of BoHV-1 and HSV-1-based viral immunotherapies, although further work in additional models is required to validate these observations.

We have historically failed to observe a correlation between viral replication capacity *in vitro* and anti-tumor activity *in vivo*.^{4,17,18,23} The goal with identifying signature genes is to provide a framework to examine whether transcriptional events could be a useful *in vitro*

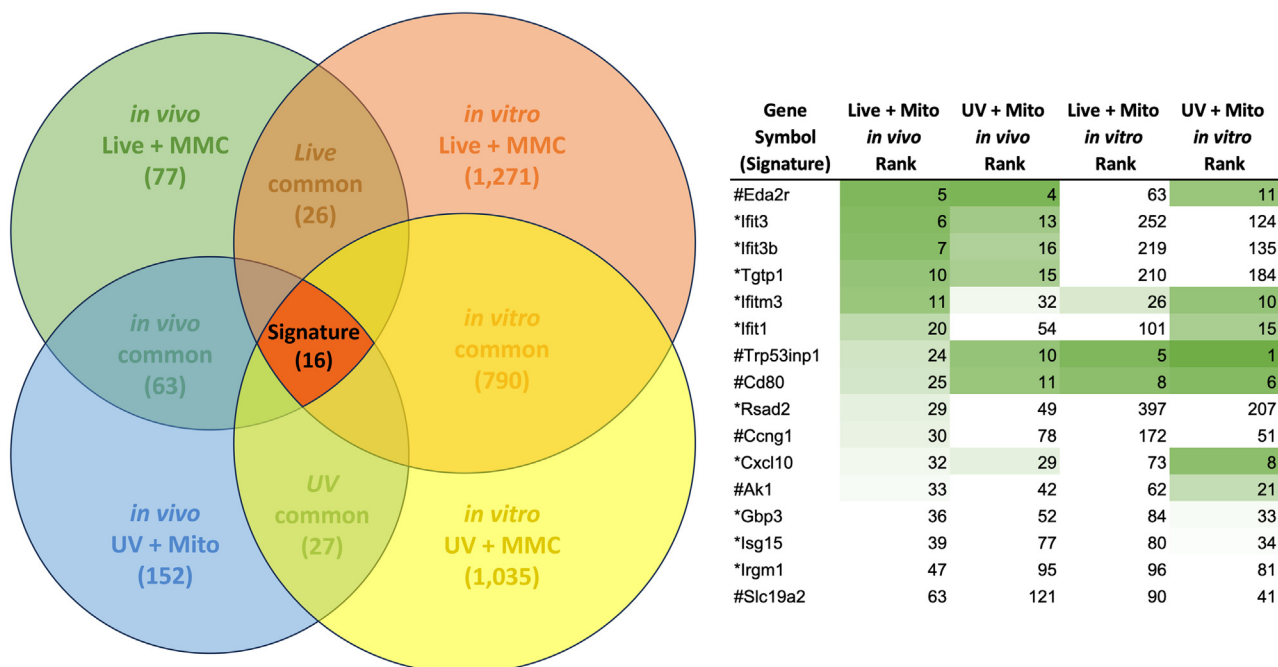


Figure 5. Schematic diagram of differential gene expression patterns in C10 cells and tumors infected *in vitro* (12 hpi) or *in vivo* (5 d post infection) with live or UV BoHV-1 in the presence of low dose mitomycin C

Values within a given set of the Venn diagram represent the number of genes differentially regulated between the indicated group and its respective mock-infected control. Signature genes are the intersection of genes differentially regulated across live BoHV-1 and UV BoHV-1 treatments, and across *in vitro* vs. *in vivo* experiments all treated with mitomycin C. The table lists the 16 signature genes and indicates their fold-change ranking within their group. *ISG. #p53-related.

screening tool for additional therapeutic regimens. Given the inherent biological diversity between tumors, it is unlikely that a specific gene set would be representative of diverse tumor types. Of interest, however, is that 10 of 16 genes within the signature gene set are ISGs, with many belonging to a subset of ISGs driven by IRF3 activation.^{9,10,59} It will be of particular interest in future studies to identify whether an IRF3 signature *in vitro* can be used to predict efficacy of a given therapeutic *in vivo*. The potential role of IRF3 is further implicated by our findings that UV-inactivated BoHV-1 retains activity as a viral immunotherapy, as our previous work in normal (untransformed cells) highlighted the role of IRF3 in responding to disruptions in homeostasis such as entry of enveloped virus particles into cells.^{5–10,60} Interestingly, while BoHV-1 replicates poorly in C10 cells,²³ live BoHV-1 induces a much larger gene signature than UV inactivated virus, suggesting that the limited replication is still of consequence to the cell response despite not affecting overall therapy efficacy.

Collectively, our findings show that equal numbers of live and UV BoHV-1 particles within our therapeutic regimen similarly control tumor growth and survival, potentially through stimulation of immune pathways activated by IRF3. While virus replication would presumably amplify innate immune signaling, large, complex DNA viruses such as herpesviruses and poxviruses encode a plethora of immune evasion genes. While we suggested several years ago that the balance between immune stimulation and immune evasion would

be an important factor in determining the therapeutic activity of a given viral immunotherapy,⁴ we were still surprised by our findings, particularly given the small number of genes induced in C10 cells and tumors with inactivated virus. Future studies with additional viral vectors and tumor cells, particularly those with validated mutations in IRF3 and other key pathways, will be informative in understanding the minimal events required for the success of a given viral immunotherapy.

MATERIALS AND METHODS

Cells

CRIB cells,⁶¹ derived from Madin-Darby bovine kidney cells to be resistant to bovine viral diarrhea virus and other pestiviruses,⁶² were generously gifted by Dr. Clinton Jones (Oklahoma State University) and cultured in DMEM supplemented with 5% fetal bovine serum (FBS) and 1% L-glutamine. C10 cells⁶³ (derived from B16 B78H1 mouse melanoma cells and expressing human Nectin-1) were generously gifted from Dr. Gary Cohen (University of Pennsylvania) and maintained in DMEM supplemented with 5% FBS, 1% L-glutamine, 100 U/mL penicillin-streptomycin, and 250 µg/mL Geneticin (Gibco Cat# 10131035).

Virus

BoHVgfp⁶⁴ was generously gifted by Dr. Günther Keil (Friedrich-Loeffler-Institut, Greifswald, Mecklenburg-Vorpommern, Germany)

Table 1. Summarized roles of the 16 signature genes

Gene	Role
<i>Eda2r</i>	alias XEDAR: p53-regulated, promoter of apoptosis, inhibitor of cell adhesion transmembrane and member of the TNF receptor superfamily ^{26,27}
<i>Ifit3</i>	forms complex to inhibit viral replication by binding viral RNA ²⁸ ; controversial role in cancer depending on cell type ²⁹
<i>Ifit3b</i>	forms complex to inhibit viral replication by binding viral RNA ²⁸ ; controversial role in cancer depending on cell type ²⁹
<i>Tgtp1</i>	alias T cell specific-GTPase; involved in response to virus; acts upstream of cellular responses to IFN alpha, beta, and gamma ³⁰
<i>Ifitm3</i>	restricts cellular entry of a variety of viruses; a pan-cancer analysis showed a positive correlation between ifitm3 expression and tumor-infiltration immune cells and immune checkpoints ³¹
<i>Ifit1</i>	forms complex to inhibit viral replication by binding viral RNA ²⁸ ; controversial role in cancer depending on cell type ²⁹
<i>Trp53inp1</i>	P53-induced, mediator antioxidant function; absence of TP53INP1 (loss of antioxidant function) favors cancer progression due to ROS ³²
<i>Cd80</i>	antigen presentation; CD80 binds both CD28 (stimulating T cells) and CTLA-4 (inhibiting T cells), can be induced by p53 in cancer ³³
<i>Rsad2</i> (viperin)	inhibits DNA and RNA viral replication ³⁴ ; increased expression correlates with a significant reduction in breast cancer patient survival ³⁵
<i>Ccng1</i>	blocks mitosis when upregulated, cell cycle regulator; transcriptional target of p53 ³⁶
<i>Cxcl10</i>	chemokine; stimulates monocytes, NK, and T cells that can attack cancer; also associated with tumor development and metastasis ³⁷
<i>Ak1</i>	ATP regulation, AK expression is downregulated in several tumors, may be related to oxidative stress; controversial, contains several consensus p53 sites ³⁸
<i>Gbp3</i>	part of the family of guanylate binding proteins; positively correlated with STING expression in human glioblastoma; differential expression from healthy cells differs among cancers ³⁹
<i>Isg15</i>	extracellular immunomodulatory cytokine that regulates cellular function by conjugating proteins; highly expressed in most tumors; evidence suggests ISG15 conjugates are pro-tumor but free ISG15 is anti-tumor ⁴⁰
<i>Irgm1</i>	immune-related GTPase; found to increase B16 cell metastasis <i>in vivo</i> and <i>in vitro</i> ⁴¹ ; negative regulator of IFN-dependent stimulation of hematopoietic stem cells ⁴²
<i>Slc19a2</i>	solute carrier for B1 (thiamine); target for activation by the p53 tumor suppressor ⁴³

and has a partial deletion in the *gl* locus and an insertion of enhanced GFP controlled by a murine cytomegalovirus promoter. CRIB cells were used to propagate and titer BoHVgfp. Virus stocks were prepared as described previously and stored at -80°C .¹⁹ For each exper-

iment, the same batch of virus was used (live or UV) keeping the concentration constant to ensure the same number of virus particles were used for each experimental condition.

UV inactivation

UV inactivation was defined to be the condition needed to reduce viral titers a minimum of 10^5 -fold, as done previously.⁵ UV inactivation of BoHV-1 was performed using a mercury lamp ultraviolet crosslinker emitting 254 nm UV-C radiation (Stratalinker). Immediately after UV treatment, plaque assays and growth curves were performed using CRIB cells to confirm UV inactivation.

Drug and antibody preparation for *in vivo* experiments

Mitomycin C powder (Sigma Cat# M4287) was dissolved in sterile water to a concentration of 2 mg/mL, and a new bottle was used for each experiment. Anti-mouse α -CTLA-4 and α -PD-L1 antibodies (BioXCell Cat# BE0131 and BE0101, respectively) were diluted to 1 mg/mL with sterile PBS.

Tumor regression study of mice bearing C10 tumors

Female C57Bl/6 mice were cared for by the McMaster University Central Animal Facility. All experiments aligned with standards from the Canadian Council on Animal Care and were approved by the Animal Research Ethics Board of McMaster University. The schematic for this experiment is outlined in Figures 2A and is based on a previously established therapeutic regimen.²³ Six- to 8-week-old C57Bl/6 female mice were implanted with 5×10^6 C10 cells resuspended in 200 μL PBS subcutaneously into the left flank. After approximately 2 weeks when tumors reached sizes between 50 and 100 mm^3 , mice were treated with 100 μg (50 μL) mitomycin C or sterile water as a vehicle control intratumorally (day 0). Every day from days 1 to 3, mice received intratumoral injections of 2×10^7 PFU live BoHV-1, an equivalent volume of UV BoHV-1, or PBS. Treated mice also received intraperitoneal injections of α -CTLA-4 and α -PD-L1 antibodies (200 μg each; 200 μL) starting on day 1 and every 3 days for 10 total doses. Tumors were measured every 3–4 days and mice were considered endpoint when tumor volumes reached 550 mm^3 .

Transcriptome profiling

For the *in vitro* transcriptome analysis, C10 cells were mock infected or infected with live or UV BoHVgfp, either in the presence of 20 $\mu\text{g}/\text{mL}$ pre-diluted mitomycin C (Sigma Cat# M5353) or DMSO (vehicle control) and RNA was harvested at 6 and 12 hpi using the RNeasy Plus Mini Kit (Qiagen Cat# 74136). The ThermoFisher Affymetrix Clariom S Mouse Assay (Cat. # 902930) was used, which provides a transcriptome-wide analysis of over 20,000 annotated genes. In summary, 12 groups were analyzed using the Clariom S Mouse Assay: C10 cells infected with live, UV BoHV-1, and mock-infected, each with or without mitomycin C, at 6 hpi and 12 hpi. This process was repeated 3 times to generate 3 biological replicates, totaling 36 samples.

For *in vivo* transcriptome analysis, C10 tumors were treated with either PBS or UV BoHV-1 with or without mitomycin C (Sigma

Cat# M4287). Transcriptome data from tumors treated with live BoHV-1 were taken from our previous study and reanalysed.²³ Tumors were harvested 5 days after treatment and homogenized in Trizol Reagent (Thermo Cat# 15-596-018). After homogenization, chloroform was added and samples were left to incubate at room temperature for 3 min. Samples were centrifuged at 12,000×g for 15 min at 4°C and the top aqueous layer was mixed with 70% ethanol in a separate tube. RNA from this mixture was isolated using the same RNeasy Plus Mini Kit, diluted to 100 ng/μL and reverse transcribed. Single-stranded cDNA was purified using magnetic beads and fragmented using UDG. The fragmented samples were hybridized to the Affymetrix Clariom S Mouse Assay, and the stained arrays were scanned to generate intensity data. All reagents for this assay were purchased from Thermo Fisher Scientific.

Tumor infiltration of immune cells

Tumors were harvested and minced with a razor blade in RPMI +10% FBS. Then, 50 μg/mL Liberase (Sigma Cat# 5401054001) was added for digestion and samples were incubated for 1 h at 37°C with constant stirring. The cell suspension was passed over a 100-micron filter and rinsed with 5 mL of RPMI +10% FBS. Cells were pelleted and ACK Lysis buffer (Quality Biological Cat# 118-156-101) was used to lyse red blood cells. Viability staining was done using the Zombie UV Fixable Viability Kit (BioLegend Cat# 423107). Cells were treated with anti-CD16/CD32 (Fc block; BD Biosciences Cat# 553141) and surface stained with fluorescently conjugated antibodies against F4/80 (BD Biosciences Cat# 565635), Ly6G (BD Biosciences Cat# 569406), CD8 (BD Biosciences Cat# 563046), CD45 (BD Biosciences Cat# 562420), CD4 (BD Biosciences Cat# 552775), CD11b (BD Biosciences Cat# 553311), CD3 (BD Biosciences Cat# 561388), and NK1.1 (BD Biosciences Cat# 550627). Cells were then intracellularly stained with anti-FoxP3 (BD Biosciences Cat# 560403). The CytoFLEX LX flow cytometer was used for data acquisition and the FlowJo Software version 10.10.0 was used for data analysis.

Statistical analysis

An unpaired t test was used to compare the means between two groups of data. Kaplan-Meier curves were used to estimate survival, and the log rank Mantel-Cox test was used to determine the difference in survival. A *p* values of less than 0.05 was considered significant. Data analyses for tumor regression and immune cell infiltration experiments were carried out using GraphPad Prism version 9.3.1. Microarray data was analyzed using the Thermo Fisher Scientific Transcriptome Analysis Console software, version 4.0.2.1.5, with SST-RMA normalization. For all transcriptome analyses, only genes with a fold-change in expression of >3 were included.

DATA AND CODE AVAILABILITY

Clariom S assay data can be found in the GEO database GSE267741.

ACKNOWLEDGMENTS

This work was supported by operating grants to K.M. from the Terry Fox Research Institute, the Cancer Research Society, and the Canadian Cancer Society. E.M.B. was the recipient of a scholarship from the Natural Sciences and Engineering Research Council of Canada.

AUTHOR CONTRIBUTIONS

Conceptualization, all authors; data curation, E.M.B, M.E.D., O.C., and S.C.; formal analysis, E.M.B, M.E.D, O.C., and K.M.; funding acquisition K.M.; investigation, E.M.B, M.E.D., and O.C.; methodology, all authors; project administration K.M.; supervision, K.M.; validation, E.M.B., M.E.D., and O.C.; visualization, E.M.B. and O.C.; writing-original draft, E.M.B.; writing-review & editing, all authors.

DECLARATION OF INTERESTS

The authors declare no conflict of interest.

SUPPLEMENTAL INFORMATION

Supplemental information can be found online at <https://doi.org/10.1016/j.omton.2024.200906>.

REFERENCES

- Shalhout, S.Z., Miller, D.M., Emerick, K.S., and Kaufman, H.L. (2023). Therapy with oncolytic viruses: progress and challenges. *Nat. Rev. Clin. Oncol.* 20, 160–177. <https://doi.org/10.1038/s41571-022-00719-w>.
- Ma, R., Li, Z., Chiocca, E.A., Caligiuri, M.A., and Yu, J. (2023). The emerging field of oncolytic virus-based cancer immunotherapy. *Trends Cancer* 9, 122–139. <https://doi.org/10.1016/j.trecan.2022.10.003>.
- Bell, J., and McFadden, G. (2014). Viruses for tumor therapy. *Cell Host Microbe* 15, 260–265. <https://doi.org/10.1016/j.chom.2014.01.002>.
- Davola, M.E., and Mossman, K.L. (2019). Oncolytic viruses: how “lytic” must they be for therapeutic efficacy? *OncImmunology* 8, e1581528. <https://doi.org/10.1080/2162402x.2019.1596006>.
- Collins, S.E., Noyce, R.S., and Mossman, K.L. (2004). Innate cellular response to virus particle entry requires IRF3 but not virus replication. *J. Virol.* 78, 1706–1717.
- Hare, D., and Mossman, K.L. (2013). Novel paradigms of innate immune sensing of viral infections. *Cytokine* 63, 219–224. <https://doi.org/10.1016/j.cyto.2013.06.001>.
- Hare, D.N., Baid, K., Dvorkin-Gheva, A., and Mossman, K.L. (2020). Virus-Intrinsic Differences and Heterogeneous IRF3 Activation Influence IFN-Independent Antiviral Protection. *iScience* 23, 101864. <https://doi.org/10.1016/j.isci.2020.101864>.
- Hare, D.N., Collins, S.E., Mukherjee, S., Loo, Y.M., Gale, M., Janssen, L.J., and Mossman, K.L. (2015). Membrane Perturbation-Associated Ca²⁺-Signaling and Incoming Genome Sensing Are Required for the Host Response to Low-Level Enveloped Virus Particle Entry. *J. Virol.* 90, 3018–3027. <https://doi.org/10.1128/jvi.02642-15>.
- Mossman, K.L., Macgregor, P.F., Rozmus, J.J., Goryachev, A.B., Edwards, A.M., and Smiley, J.R. (2001). Herpes simplex virus triggers and then disarms a host antiviral response. *J. Virol.* 75, 750–758.
- Noyce, R.S., Taylor, K., Ciechonska, M., Collins, S.E., Duncan, R., and Mossman, K.L. (2011). Membrane perturbation elicits an IRF3-dependent, interferon-independent antiviral response. *J. Virol.* 85, 10926–10931. <https://doi.org/10.1128/JVI.00862-11>.
- Holm, C.K., Jensen, S.B., Jakobsen, M.R., Cheshenko, N., Horan, K.A., Moeller, H.B., Gonzalez-Dosal, R., Rasmussen, S.B., Christensen, M.H., Yarovinsky, T.O., et al. (2012). Virus-cell fusion as a trigger of innate immunity dependent on the adaptor STING. *Nat. Immunol.* 13, 737–743. <https://doi.org/10.1038/ni.2350>.
- Dai, P., Wang, W., Yang, N., Serna-Tamayo, C., Ricca, J.M., Zamarin, D., Shuman, S., Merghoub, T., Wolchok, J.D., and Deng, L. (2017). Intratumoral delivery of inactivated modified vaccinia virus Ankara (iMVA) induces systemic antitumor immunity via STING and Batf3-dependent dendritic cells. *Sci. Immunol.* 2, eaal1713. <https://doi.org/10.1126/sciimmunol.aal1713>.
- Wang, W., Liu, S., Dai, P., Yang, N., Wang, Y., Giese, R.A., Merghoub, T., Wolchok, J., and Deng, L. (2021). Elucidating mechanisms of antitumor immunity mediated by live oncolytic vaccinia and heat-inactivated vaccinia. *J. Immunother. Cancer* 9, e002569. <https://doi.org/10.1136/jitc-2021-002569>.
- Samudio, I., Rezvani, K., Shaim, H., Hofs, E., Ngom, M., Bu, L., Liu, G., Lee, J.T.C., Imren, S., Lam, V., et al. (2016). UV-inactivated HSV-1 potently activates NK cell killing of leukemic cells. *Blood* 127, 2575–2586. <https://doi.org/10.1182/blood-2015-04-639088>.

15. Samudio, I., Hofs, E., Cho, B., Li, M., Bolduc, K., Bu, L., Liu, G., Lam, V., Rennie, P., Jia, W., et al. (2019). UV Light-inactivated HSV-1 Stimulates Natural Killer Cell-induced Killing of Prostate Cancer Cells. *J. Immunother.* *42*, 162–174. <https://doi.org/10.1097/CJI.0000000000000261>.
16. Froechlich, G., Caiazza, C., Gentile, C., D'Alise, A.M., De Lucia, M., Langone, F., Leoni, G., Cotugno, G., Scisciola, V., Nicosia, A., et al. (2020). Integrity of the Antiviral STING-mediated DNA Sensing in Tumor Cells Is Required to Sustain the Immunotherapeutic Efficacy of Herpes Simplex Oncolytic Virus. *Cancers* *12*, 3407. <https://doi.org/10.3390/cancers12113407>.
17. Sobol, P.T., Boudreau, J.E., Stephenson, K., Wan, Y., Lichty, B.D., and Mossman, K.L. (2011). Adaptive antiviral immunity is a determinant of the therapeutic success of oncolytic virotherapy. *Mol. Ther.* *19*, 335–344. <https://doi.org/10.1038/mt.2010.264>.
18. Workenhe, S.T., Simmons, G., Pol, J.G., Lichty, B.D., Halford, W.P., and Mossman, K.L. (2014). Immunogenic HSV-mediated oncolysis shapes the antitumor immune response and contributes to therapeutic efficacy. *Mol. Ther.* *22*, 123–131. <https://doi.org/10.1038/mt.2013.238>.
19. Cuddington, B.P., Dyer, A.L., Workenhe, S.T., and Mossman, K.L. (2013). Oncolytic bovine herpesvirus type 1 infects and kills breast tumor cells and breast cancer-initiating cells irrespective of tumor subtype. *Cancer Gene Ther.* *20*, 282–289. <https://doi.org/10.1038/cgt.2013.18>.
20. Cuddington, B.P., and Mossman, K.L. (2014). Permissiveness of Human Cancer Cells to Oncolytic Bovine Herpesvirus 1 Is Mediated in Part by KRAS Activity. *J. Virol.* *88*, 6885–6895. <https://doi.org/10.1128/JVI.00849-14>.
21. Cuddington, B.P., and Mossman, K.L. (2015). Oncolytic bovine herpesvirus type 1 as a broad spectrum cancer therapeutic. *Curr. Opin. Virol.* *13*, 11–16. <https://doi.org/10.1016/j.coviro.2015.03.010>.
22. Rodrigues, R., Cuddington, B., and Mossman, K. (2010). Bovine herpesvirus type 1 as a novel oncolytic virus. *Cancer Gene Ther.* *17*, 344–355. [cgt200977 \[pii\]. https://doi.org/10.1038/cgt.2009.77](https://doi.org/10.1038/cgt.2009.77).
23. Davola, M.E., Cormier, O., Vito, A., El-Sayes, N., Collins, S., Salem, O., Revill, S., Ask, K., Wan, Y., and Mossman, K. (2023). Oncolytic BHV-1 Is Sufficient to Induce Immunogenic Cell Death and Synergizes with Low-Dose Chemotherapy to Dampen Immunosuppressive T Regulatory Cells. *Cancers* *15*, 1295. <https://doi.org/10.3390/cancers15041295>.
24. El-Sayes, N., Vito, A., Salem, O., Workenhe, S.T., Wan, Y., and Mossman, K. (2022). A Combination of Chemotherapy and Oncolytic Virotherapy Sensitizes Colorectal Adenocarcinoma to Immune Checkpoint Inhibitors in a cDC1-Dependent Manner. *Int. J. Mol. Sci.* *23*, 1754. <https://doi.org/10.3390/ijms23031754>.
25. Workenhe, S.T., Nguyen, A., Bakshshinyan, D., Wei, J., Hare, D.N., MacNeill, K.L., Wan, Y., Oberst, A., Bramson, J.L., Nasir, J.A., et al. (2020). De novo necroptosis creates an inflammatory environment mediating tumor susceptibility to immune checkpoint inhibitors. *Commun. Biol.* *3*, 645. <https://doi.org/10.1038/s42003-020-01362-w>.
26. Zhang, X., Zhang, D., Sun, X., Li, S., Sun, Y., and Zhai, H. (2021). Tumor Suppressor Gene XEDAR Promotes Differentiation and Suppresses Proliferation and Migration of Gastric Cancer Cells Through Upregulating the RELA/LXR α Axis and Deactivating the Wnt/ β -Catenin Pathway. *Cell Transplant.* *30*, 963689721996346. <https://doi.org/10.1177/0963689721996346>.
27. Tanikawa, C., Ri, C., Kumar, V., Nakamura, Y., and Matsuda, K. (2010). Crosstalk of EDA-A2/XEDAR in the p53 signaling pathway. *Mol. Cancer Res.* *8*, 855–863. <https://doi.org/10.1158/1541-7786.MCR-09-0484>.
28. Fleith, R.C., Mears, H.V., Leong, X.Y., Sanford, T.J., Emmott, E., Graham, S.C., Mansur, D.S., and Sweeney, T.R. (2018). IFIT3 and IFIT2/3 promote IFIT1-mediated translation inhibition by enhancing binding to non-self RNA. *Nucleic Acids Res.* *46*, 5269–5285. <https://doi.org/10.1093/nar/gky191>.
29. Pidugu, V.K., Pidugu, H.B., Wu, M.M., Liu, C.J., and Lee, T.C. (2019). Emerging Functions of Human IFIT Proteins in Cancer. *Front. Mol. Biosci.* *6*, 148. <https://doi.org/10.3389/fmolb.2019.00148>.
30. Carlow, D.A., Teh, S.J., and Teh, H.S. (1998). Specific antiviral activity demonstrated by TGTP, a member of a new family of interferon-induced GTPases. *J. Immunol.* *161*, 2348–2355.
31. Cai, Y., Ji, W., Sun, C., Xu, R., Chen, X., Deng, Y., Pan, J., Yang, J., Zhu, H., and Mei, J. (2021). Interferon-Induced Transmembrane Protein 3 Shapes an Inflamed Tumor Microenvironment and Identifies Immuno-Hot Tumors. *Front. Immunol.* *12*, 704965. <https://doi.org/10.3389/fimmu.2021.704965>.
32. Seillier, M., Peugot, S.J.N., and Carrier, A. (2012). Antioxidant Role of P53 and of its Target TP53INP1 (InTech). <https://doi.org/10.5772/50790>.
33. Alibo, E., Mollaoglu, G., Dhainaut, M., Zhao, R., Rose, S., Baccarini, A., Parsons, R., and Brown, B.D. (2021). P53 is a direct regulator of the immune co-stimulatory molecule CD80. Preprint at bioRxiv. <https://doi.org/10.1101/2021.05.24.445214>.
34. Jang, J.S., Lee, J.H., Jung, N.C., Park, S.Y., Park, S.Y., Yoo, J.Y., Song, J.Y., Seo, H.G., Lee, H.S., and Lim, D.S. (2018). Rsd2 is necessary for mouse dendritic cell maturation via the IRF7-mediated signaling pathway. *Cell Death Dis.* *9*, 823. <https://doi.org/10.1038/s41419-018-0889-y>.
35. Lewis, M.W., Wisniewska, K., King, C.M., Li, S., Coffey, A., Kelly, M.R., Regner, M.J., and Franco, H.L. (2022). Enhancer RNA Transcription Is Essential for a Novel CSF1 Enhancer in Triple-Negative Breast Cancer. *Cancers* *14*, 1852. <https://doi.org/10.3390/cancers14071852>.
36. Gordon, E.M., Ravicz, J.R., Liu, S., Chawla, S.P., and Hall, F.L. (2018). Cell cycle checkpoint control: The cyclin G1/Mdm2/p53 axis emerges as a strategic target for broad-spectrum cancer gene therapy - A review of molecular mechanisms for oncologists. *Mol. Clin. Oncol.* *9*, 115–134. <https://doi.org/10.3892/mco.2018.1657>.
37. Liu, M., Guo, S., and Stiles, J.K. (2011). The emerging role of CXCL10 in cancer (Review). *Oncol. Lett.* *2*, 583–589. <https://doi.org/10.3892/ol.2011.300>.
38. Klepinin, A., Zhang, S., Klepinina, L., Rebane-Klemm, E., Terzic, A., Kaambre, T., and Dzeja, P. (2020). Adenylate Kinase and Metabolic Signaling in Cancer Cells. *Front. Oncol.* *10*, 660. <https://doi.org/10.3389/fonc.2020.00660>.
39. Xu, H., Jin, J., Chen, Y., Wu, G., Zhu, H., Wang, Q., Wang, J., Li, S., Grigore, F.N., Ma, J., et al. (2022). GBP3 promotes glioblastoma resistance to temozolomide by enhancing DNA damage repair. *Oncogene* *41*, 3876–3885. <https://doi.org/10.1038/s41388-022-02397-5>.
40. Desai, S.D. (2015). ISG15: A double edged sword in cancer. *Oncolimmunology* *4*, e1052935. <https://doi.org/10.1080/2162402X.2015.1052935>.
41. Tian, L., Li, L., Xing, W., Li, R., Pei, C., Dong, X., Fu, Y., Gu, C., Guo, X., Jia, Y., et al. (2015). IRGM1 enhances B16 melanoma cell metastasis through PI3K-Rac1 mediated epithelial mesenchymal transition. *Sci. Rep.* *5*, 12357. <https://doi.org/10.1038/srep12357>.
42. King, K.Y., Baldrige, M.T., Weksberg, D.C., Chambers, S.M., Lukov, G.L., Wu, S., Boles, N.C., Jung, S.Y., Qin, J., Liu, D., et al. (2011). Irgm1 protects hematopoietic stem cells by negative regulation of IFN signaling. *Blood* *118*, 1525–1533. <https://doi.org/10.1182/blood-2011-01-328682>.
43. Lai, Y. (2013). Membrane transporters and the diseases corresponding to functional defects. In Woodhead Publishing Series in Biomedicine, Transporters in Drug Discovery and Development, Y. Lai, ed. (Woodhead Publishing), pp. 1–146. <https://doi.org/10.1533/9781908818287.1>.
44. Ling, A.L., and Chiocca, E.A. (2024). Oncolytic immunoactivation associates with survival in a glioblastoma clinical trial. *Neuro Oncol.* *26*, 209–210. <https://doi.org/10.1093/neuonc/noad216>.
45. Ling, A.L., Solomon, I.H., Landivar, A.M., Nakashima, H., Woods, J.K., Santos, A., Masud, N., Fell, G., Mo, X., Yilmaz, A.S., et al. (2023). Clinical trial links oncolytic immunoactivation to survival in glioblastoma. *Nature* *623*, 157–166. <https://doi.org/10.1038/s41586-023-06623-2>.
46. Ogbomo, H., Zemp, F.J., Lun, X., Zhang, J., Stack, D., Rahman, M.M., McFadden, G., Mody, C.H., and Forsyth, P.A. (2013). Myxoma virus infection promotes NK lysis of malignant gliomas in vitro and in vivo. *PLoS One* *8*, e66825. <https://doi.org/10.1371/journal.pone.0066825>.
47. Zamarin, D., Holmggaard, R.B., Subudhi, S.K., Park, J.S., Mansour, M., Palese, P., Merghoub, T., Wolchok, J.D., and Allison, J.P. (2014). Localized oncolytic virotherapy overcomes systemic tumor resistance to immune checkpoint blockade immunotherapy. *Sci. Transl. Med.* *6*, 226ra32. <https://doi.org/10.1126/scitranslmed.3008095>.
48. Wang, Y., Jin, J., Li, Y., Zhou, Q., Yao, R., Wu, Z., Hu, H., Fang, Z., Dong, S., Cai, Q., et al. (2022). NK cell tumor therapy modulated by UV-inactivated oncolytic herpes simplex virus type 2 and checkpoint inhibitors. *Transl. Res.* *240*, 64–86. <https://doi.org/10.1016/j.trsl.2021.10.006>.

49. Ma, Y., Zhang, Y., and Zhu, L. (2021). Role of neutrophils in acute viral infection. *Immun. Inflamm. Dis.* 9, 1186–1196. <https://doi.org/10.1002/iid3.500>.
50. Jenne, C.N., Wong, C.H.Y., Zemp, F.J., McDonald, B., Rahman, M.M., Forsyth, P.A., McPadden, G., and Kubes, P. (2013). Neutrophils recruited to sites of infection protect from virus challenge by releasing neutrophil extracellular traps. *Cell Host Microbe* 13, 169–180. <https://doi.org/10.1016/j.chom.2013.01.005>.
51. Minott, J.A., van Vloten, J.P., Chan, L., Mehrani, Y., Bridle, B.W., and Karimi, K. (2022). The Role of Neutrophils in Oncolytic Orf Virus-Mediated Cancer Immunotherapy. *Cells* 11, 2858. <https://doi.org/10.3390/cells11182858>.
52. Workenhe, S.T., Pol, J.G., Lichty, B.D., Cummings, D.T., and Mossman, K.L. (2013). Combining oncolytic HSV-1 with immunogenic cell death-inducing drug mitoxantrone breaks cancer immune tolerance and improves therapeutic efficacy. *Cancer Immunol. Res.* 1, 309–319. <https://doi.org/10.1158/2326-6066.CIR-13-0059-T>.
53. Winkler, M.T., Doster, A., and Jones, C. (1999). Bovine herpesvirus 1 can infect CD4(+) T lymphocytes and induce programmed cell death during acute infection of cattle. *J. Virol.* 73, 8657–8668. <https://doi.org/10.1128/JVI.73.10.8657-8668.1999>.
54. Kang, S.G., Chung, H., Yoo, Y.D., Lee, J.G., Choi, Y.I., and Yu, Y.S. (2001). Mechanism of growth inhibitory effect of Mitomycin-C on cultured human retinal pigment epithelial cells: apoptosis and cell cycle arrest. *Curr. Eye Res.* 22, 174–181. <https://doi.org/10.1076/ceyr.22.3.174.5513>.
55. Abbas, T., Olivier, M., Lopez, J., Houser, S., Xiao, G., Kumar, G.S., Tomasz, M., and Bargonetti, J. (2002). Differential activation of p53 by the various adducts of mitomycin C. *J. Biol. Chem.* 277, 40513–40519. <https://doi.org/10.1074/jbc.M205495200>.
56. Song, B., Shiromoto, Y., Minakuchi, M., and Nishikura, K. (2022). The role of RNA editing enzyme ADAR1 in human disease. *Wiley Interdiscip. Rev. RNA* 13, e1665. <https://doi.org/10.1002/wrna.1665>.
57. Lamers, M.M., van den Hoogen, B.G., and Haagmans, B.L. (2019). ADAR1: "Editor-in-Chief" of Cytoplasmic Innate Immunity. *Front. Immunol.* 10, 1763. <https://doi.org/10.3389/fimmu.2019.01763>.
58. Cheng, S.Y., Seo, J., Huang, B.T., Napolitano, T., and Champeil, E. (2016). Mitomycin C and decarbamoyl mitomycin C induce p53-independent p21WAF1/CIP1 activation. *Int. J. Oncol.* 49, 1815–1824. <https://doi.org/10.3892/ijo.2016.3703>.
59. Grandvaux, N., Servant, M.J., tenOever, B., Sen, G.C., Balachandran, S., Barber, G.N., Lin, R., and Hiscott, J. (2002). Transcriptional profiling of interferon regulatory factor 3 target genes: direct involvement in the regulation of interferon-stimulated genes. *J. Virol.* 76, 5532–5539. <https://doi.org/10.1128/jvi.76.11.5532-5539.2002>.
60. Collins, S.E., and Mossman, K.L. (2014). Danger, diversity and priming in innate antiviral immunity. *Cytokine Growth Factor Rev.* 25, 525–531. <https://doi.org/10.1016/j.cytogfr.2014.07.002>.
61. Workman, A., and Jones, C. (2010). Productive infection and bICP0 early promoter activity of bovine herpesvirus 1 are stimulated by E2F1. *J. Virol.* 84, 6308–6317. <https://doi.org/10.1128/JVI.00321-10>.
62. Flores, E.F., and Donis, R.O. (1995). Isolation of a mutant MDBK cell line resistant to bovine viral diarrhoea virus infection due to a block in viral entry. *Virology* 208, 565–575. <https://doi.org/10.1006/viro.1995.1187>.
63. Miller, C.G., Krummenacher, C., Eisenberg, R.J., Cohen, G.H., and Fraser, N.W. (2001). Development of a syngenic murine B16 cell line-derived melanoma susceptible to destruction by neuroattenuated HSV-1. *Mol. Ther.* 3, 160–168. <https://doi.org/10.1006/mthe.2000.0240>.
64. Keil, G.M., Höhle, C., Giesow, K., and König, P. (2005). Engineering glycoprotein B of bovine herpesvirus 1 to function as transporter for secreted proteins: a new protein expression approach. *J. Virol.* 79, 791–799. <https://doi.org/10.1128/JVI.79.2.791-799.2005>.